Supplementary material for

Enhanced electrically and thermally conductive free-standing graphene films with two-dimensional copper nanosheets as catalyst and bridge

Huangqing Ye,[a] Jiahui Chen,[b] Yougen Hu,[c] Yunming Li,[d] Yu Wang,[a]* Xian-Zhu Fu,[b]* Rong Sun[c]*

[a] International Collaborative Laboratory of 2D Materials for Optoelectronics Science and Technology of Ministry of Education, Institute of Microscale Optoelectronics, Shenzhen University, Shenzhen, 518060, China.

[b] College of Materials Science and Engineering, Shenzhen University, Shenzhen 518055, China.

[c] Shenzhen Institutes of Advanced Technology, Chinese Academy of Sciences, Shenzhen 518055, China.

[d] School of New Energy Science and Engineering, Xinyu University, Xinyu 338004, China.

Corresponding author:

* Yu Wang, E-mail address: wangyu@szu.edu.cn;

* Xian-Zhu Fu, E-mail address: xz.fu@szu.edu.cn;

* Rong Sun, E-mail address: rong.sun@siat.ac.cn.

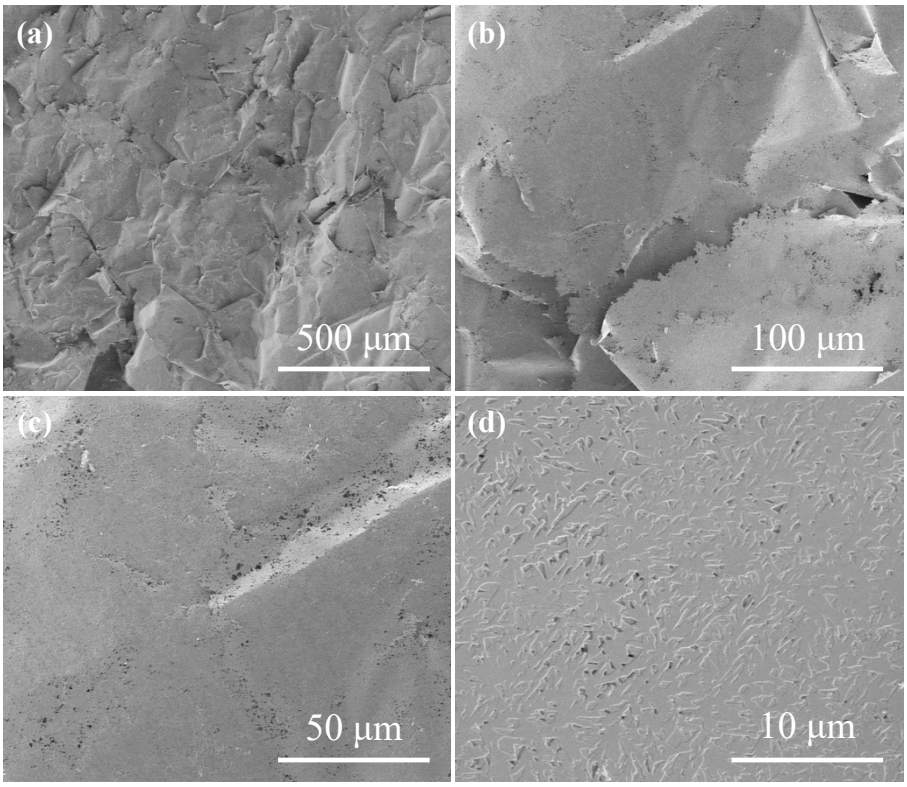

Fig. S1 SEM images of the as-prepared two-dimensional copper under different magnifications.

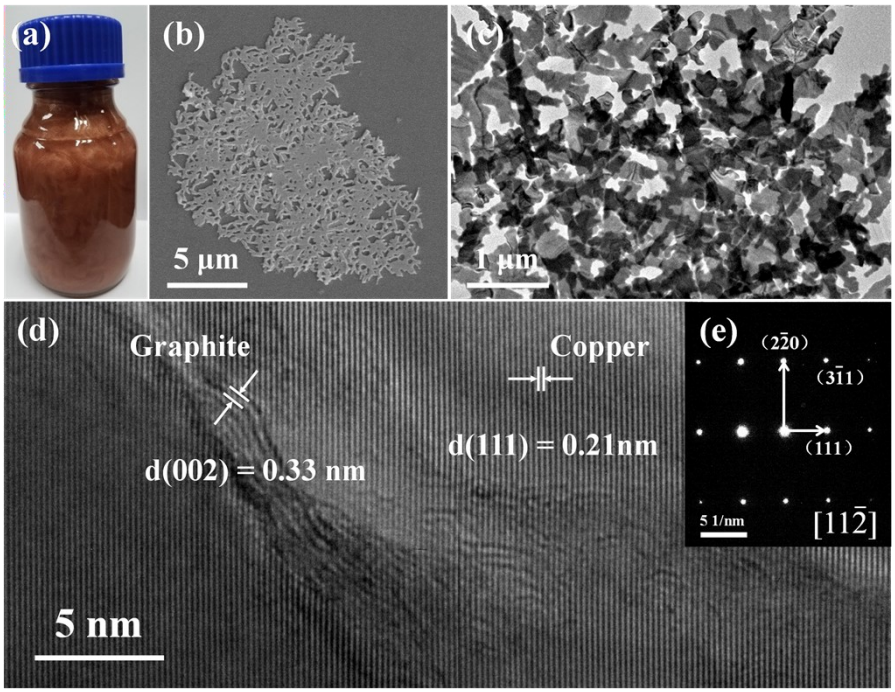

Fig. S2 (a) Optical, (b) SEM, and (c, d) HRTEM images of the two-dimensional copper after a certain dispersion process. (e) Selected area electron diffraction analysis of (d).

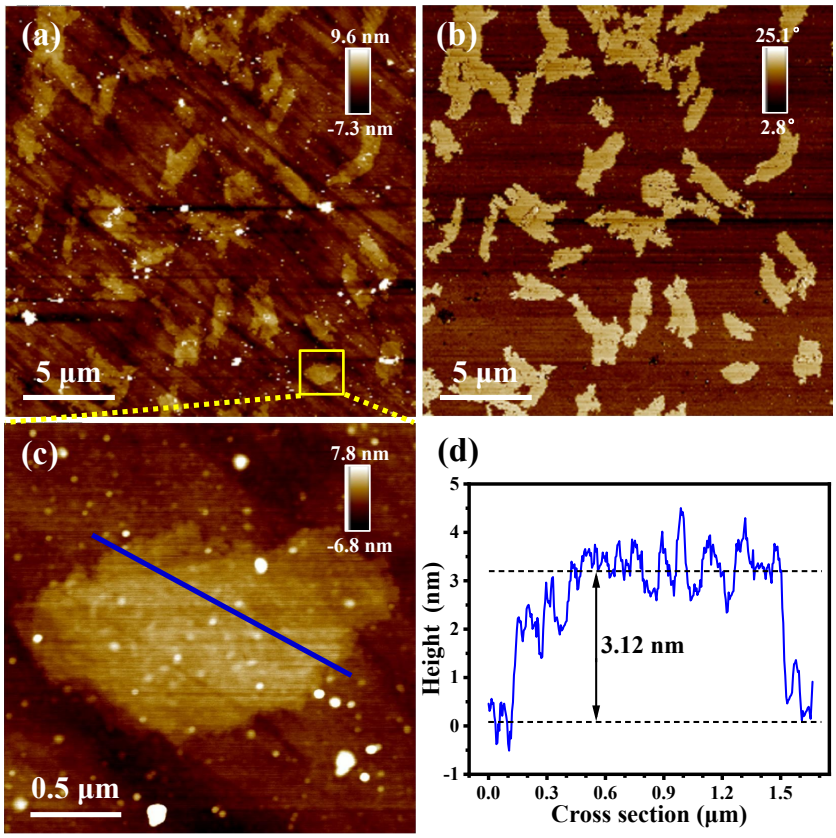

Fig. S3 AFM characterizations of the as-prepared copper after dispersion: (a, c) height and (b) phase images; (d) height profiles of a typical two-dimensional structure in (c).

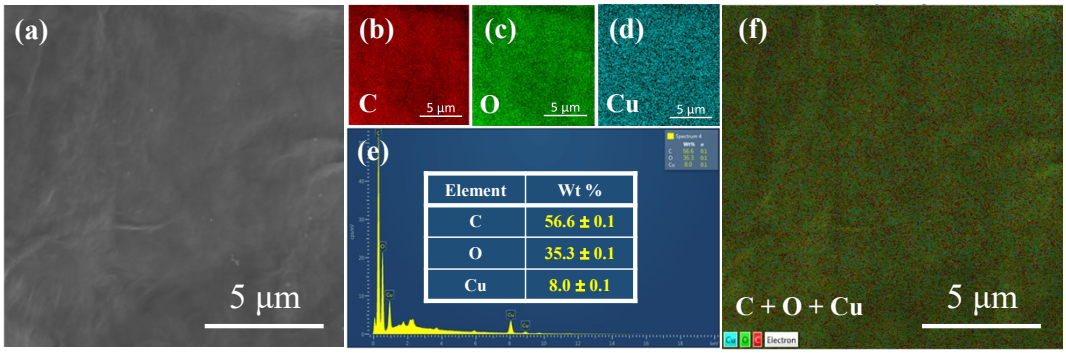

Fig. S4 Typical (a) SEM and (b–f) SEM–EDS mapping images of Cu/GO films.

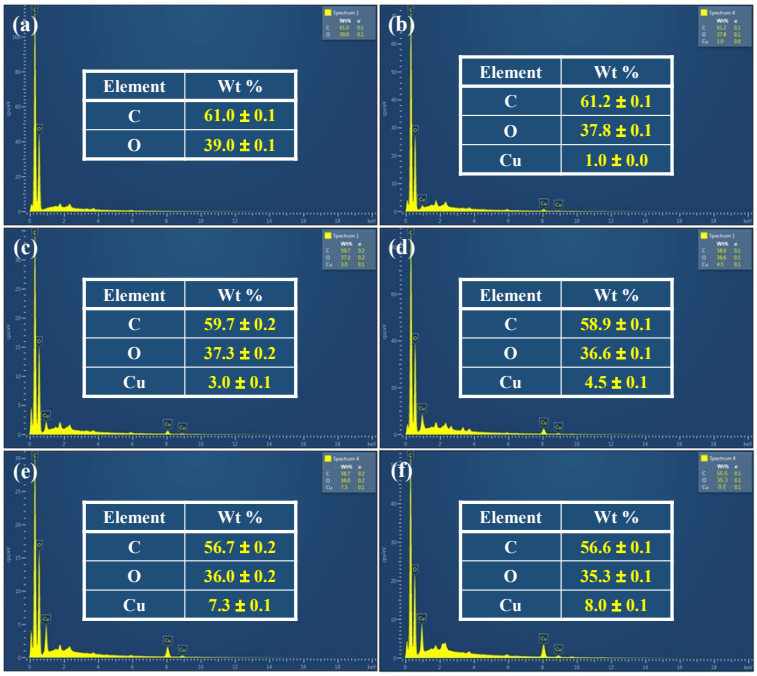

Fig. S5 Elemental content analysis via SEM-EDS: (a) GO; (b) Cu/GO-1; (c) Cu/GO-2; (d) Cu/GO-3; (e) Cu/GO-4; and (f) Cu/GO-5.

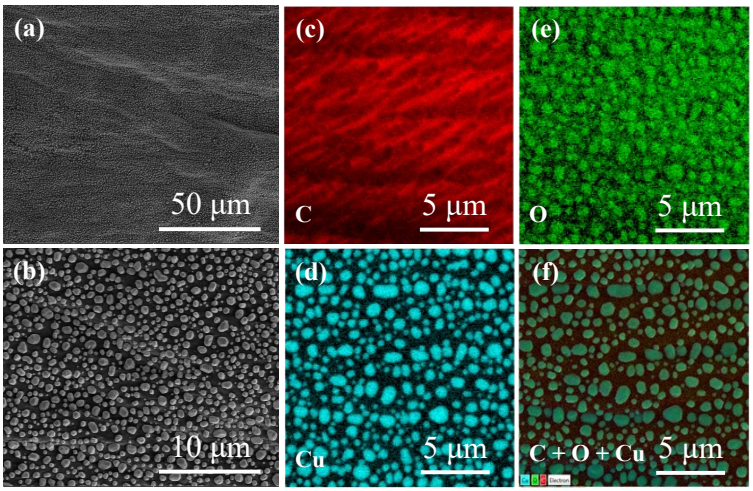

Fig. S6 (a, b) SEM images and (c-f) SEM-EDS mapping images of the Cu/rGO film prepared through annealing at 1000 °C.

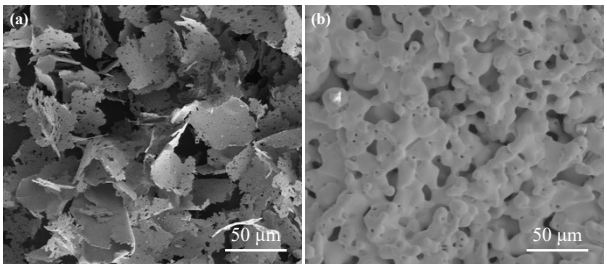

Fig. S7 SEM images of the two-dimensional copper after annealing at (a) 900 and (b) 1000 °C.

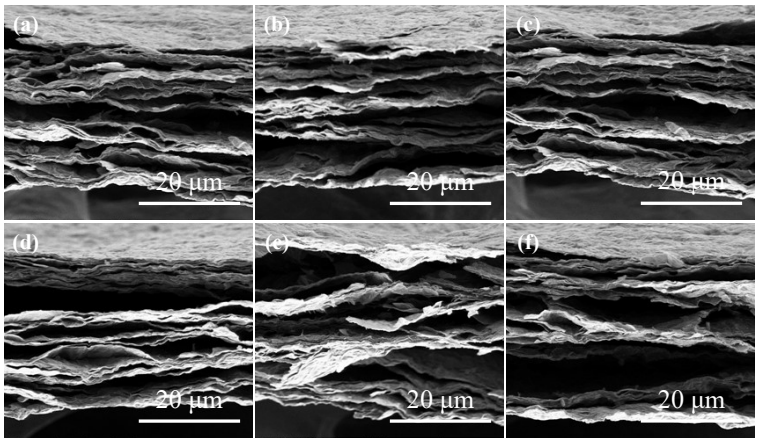

Fig. S8 SEM images of the cross-sections of the as-prepared films: (a) rGO; (b) Cu/rGO-1; (c) Cu/rGO-2; (d) Cu/rGO-3; (e) Cu/rGO-4; and (f) Cu/rGO-5.

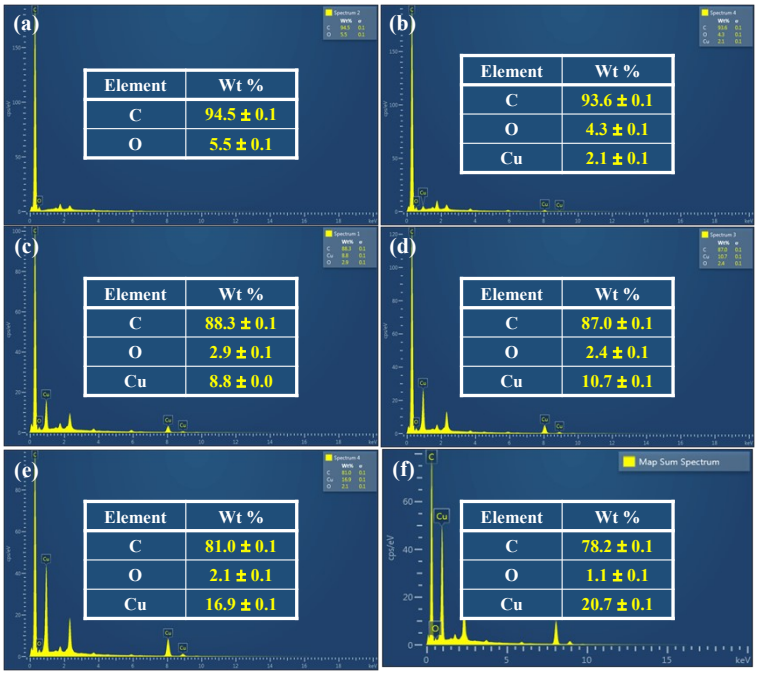

Fig. S9 Elemental content analysis through SEM–EDS: (a) rGO; (b) Cu/rGO-1; (c) Cu/rGO-2; (d) Cu/rGO-3; (e) Cu/rGO-4; and (f) Cu/rGO-5.

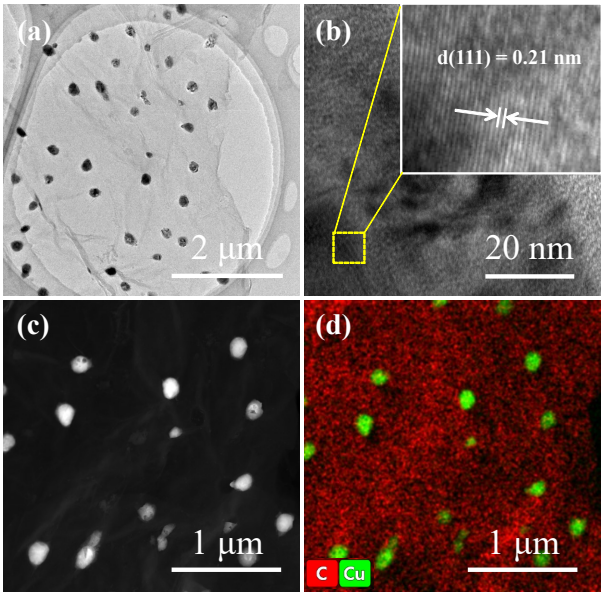

Fig. S10 (a, b) HRTEM, (c) HAADF-STEM, and (d) HAADF-STEM-EDS mapping images of typical Cu/rGO.

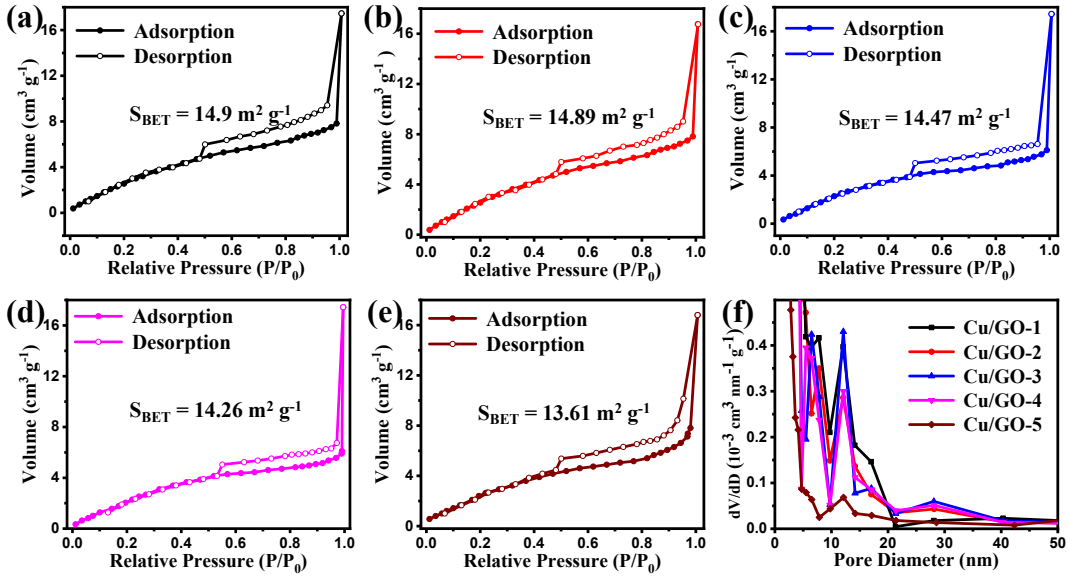

Fig. S11 Nitrogen adsorption-desorption isotherms of (a) Cu/GO-1, (b) Cu/GO-2, (c) Cu-GO-3, (d) Cu/GO-4, (e) Cu/GO-5, and corresponding (e) pore size distributions.

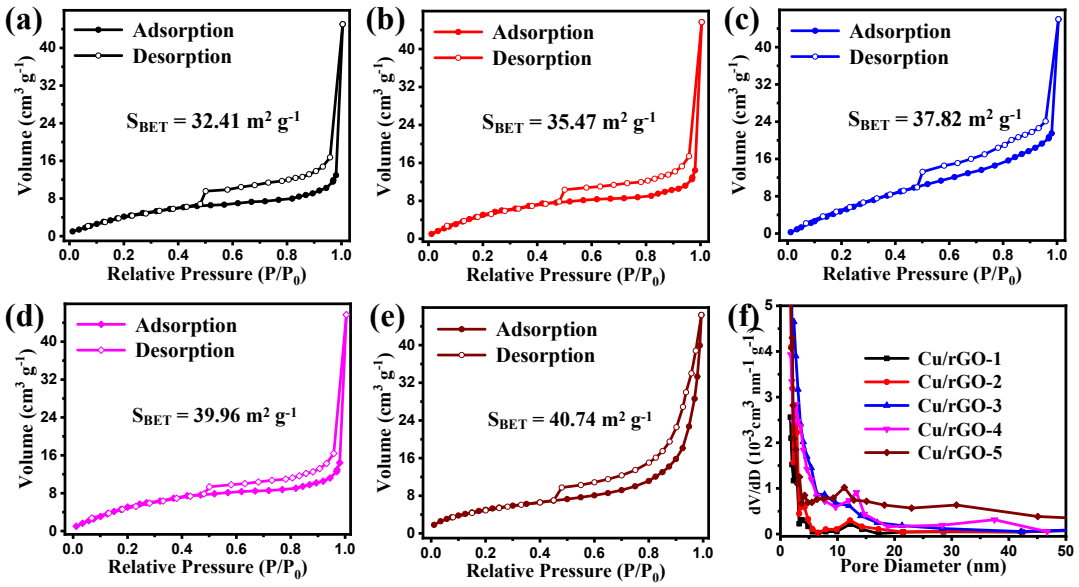

Fig. S12 Nitrogen adsorption-desorption isotherms of (a) Cu/rGO-1, (b) Cu/rGO-2, (c) Cu-rGO-3, (d) Cu/rGO-4, (e) Cu/rGO-5, and corresponding (e) pore size distributions.

Table S1 Comparative summary of thermal conductivity of graphene-based composite films.

Films	Fabrication Method	Reduction Method Post-Treatment	Thermal Measurement	Thermal conductivity (W m^{-1} K^{-1})	Refer.
Cu/rGO	Vacuum filtration	Annealed at 900 °C for 2 h	Laser flash	859	This work
N-Gr	Vacuum filtration	Annealed at 800 °C for 8 h	Laser flash	542.9	1
Gr/Cu/Gr	Chemical vapor deposition	/	Laser flash	376.4	2
rGO	Vacuum filtration	graphitization at 2600 °C for 4 h	Laser flash	803.1	3
Graphene	Vacuum filtration	dried at 105 °C for 3 h	Laser flash	112	4
Graphite	Vacuum filtration	annealed at 340 °C for 2 h	Laser flash	190	5

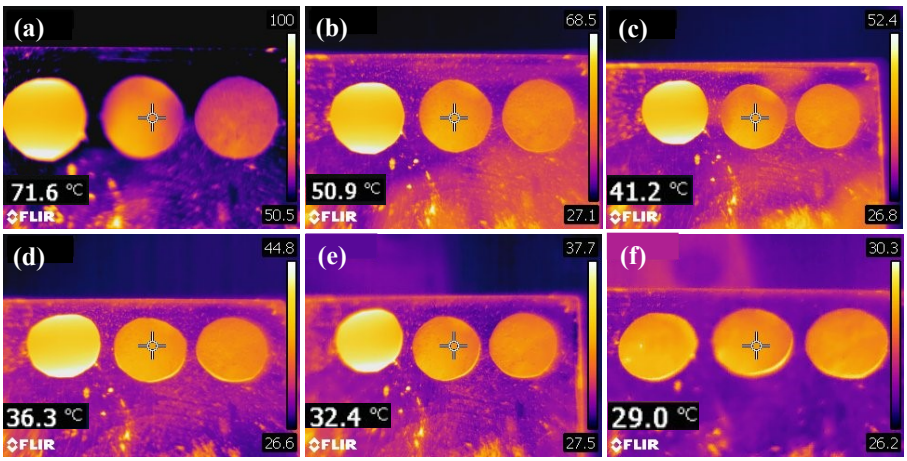

Fig. S13 Infrared thermal images of graphene films under different time: (a) 20 s, (b) 40 s, (c) 60 s, (d) 80 s, (e) 100 s, and (f) 120 s.

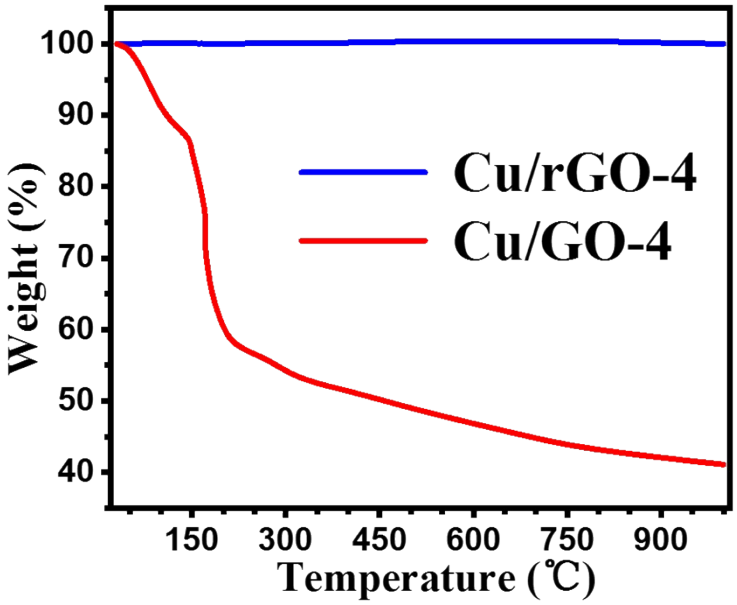

Fig. S14 TGA curves of Cu/GO-4 and Cu/rGO-4.

References

1. C.-C. Hsieh and W.-R. Liu, *Carbon*, 2017, **118**, 1-7.
2. P. Goli, H. Ning, X. Li, C. Y. Lu, K. S. Novoselov and A. A. Balandin, *Nano Letters*, 2014, **14**, 1497-1503.
3. S. Lin, S. Ju, J. Zhang, G. Shi, Y. He and D. Jiang, *RSC Advances*, 2019, **9**, 1419-1427.
4. Q. Liang, X. Yao, W. Wang, Y. Liu and C. P. Wong, *ACS Nano*, 2011, **5**, 2392-2401.
5. J. Xiang and L. T. Drzal, *Carbon*, 2011, **49**, 773-778.